Journal of JSEM, Vol.11, Special Issue (2011) SS267-SS271

Anodization of the Inner Wall of the Microchannel Formed in Sintered Aluminum Body

Masashi ISHIDA[1], Tatsuya OHMI[2], Masatoshi SAKAIRI[2] and Manabu IGUCHI[2]

[1]Graduate School of Engineering, Hokkaido University, Sapporo 060-8628, Japan
[2]Faculty of Engineering, Hokkaido University, Sapporo 060-8628, Japan

(*Received 7 January 2011; received in revised form 27 May 2011; accepted 5 June 2011*)

Abstract
A fabrication method of a nanoporous anodic alumina film on the inner wall of a microchannel was investigated. An open microchannel was produced by a powder-metallurgical microchanneling process using Al as a body metal and Zn as a sacrificial-core metal. However, the cross-sectional area of the microchannel was larger than that of the sacrificial core; it increased as the compacting pressure increased. The nanoporous alumina film was produced by anodic oxidation of the inner wall of the microchannel.

Key words
Microchannel, Powder Metallurgy, Anodic Oxidation, Aluminum-Zinc Alloy, Nanoporous Structure

1. Introduction

In recent years, many environmental and resource problems have become extremely serious. For example, there are global heating, acid rain, ozone depletion and decreasing of the recoverable reserves of the fossil fuel and the metallic resources. A catalytic research has become more important for solving these problems. Specifically, it is required to search high-performance catalysts which replace hard-to-find metallic catalysts and to develop catalyst supports which get great performance out of the catalysts. Based on this perspective, we have focused on a thin channel called microchannel. A high specific surface area due to the microchannel structure with a characteristic dimension from several to several hundreds μm and high heat conductivity of metallic materials permits high efficiency of the catalytic reaction and precise temperature control.

In many cases, precision machining or photo-etching is used to produce microchannels. However, these processes need complicated and exact work to produce metallic microchannel devices. Thus, the processing time and cost increase remarkably. [1]

Recently, we reported our research about formation of a nanoporous anodic oxide film on the inner wall of a microchannel in a titanium body. [2] The microchannel was produced by a powder-metallurgical microchanneling process. In this process, a metal powder compact containing a metallic sacrificial core is sintered. During sintering, molten sacrificial-core metal migrates to the metal powder region by infiltration and/or diffusion, and then the microchannel is produced. [3-6] This microchanneling process is simple and low cost. An open microchannel lined with a Ti-Al alloy layer was produced when titanium and aluminum were used as the body metal and the sacrificial-core metal, respectively.

A nanoporous oxide film increased the specific surface area of the inner wall of the microchannel tremendously. In addition, titanium oxide excels at heat resistance and corrosion resistance. These properties are suitable for the catalyst support.

Aluminum is a representative metal which produces the nanoporous anodic oxide film. The heat conductivity of aluminum is about ten times higher than that of titanium. It permits precision temperature control in the microreactors. Furthermore, aluminum density is about 0.6 times titanium density. In addition, aluminum is an inexpensive common metal.

In this study, we investigated the anodic oxidation of the inner wall of the microchannel produced in an aluminum body.

2. Experiments

2.1 Preparation of microchanneled specimens

We used aluminum as the body metal and zinc as the sacrificial-core metal. This combination has been reported to produce a microchannel [7]. Figure 1 shows an Al-Zn binary alloy phase diagram [8]. The melting point of aluminum is 200 K higher than that of zinc.

A body metal powder containing a sacrificial-core wire was uniaxially compressed at room temperature. Aluminum powder was used as the body metal powder, and a zinc wire 500 μm in diameter and 15 mm in length was used as the sacrificial core. The compacting pressure was 79.5, 159 or 318 MPa. The shape of the resulted compact specimen was a columnar 20 mm in diameter and 5 mm in height as shown in Fig. 2.

After that, the compact specimen was sintered in the following manner; the compact specimen was heated at a constant rate of 0.2 K/s from room temperature to 873 K, kept at 873 K for 9.0 ks and then furnace-cooled at 0.4 K/s.

The porosity of the body-metal part of the specimen before sintering was calculated by the following equation;

$$X_c = (1 - \frac{(M_c - M_s)}{\rho_{Al}(V_c - V_s)}) \times 100 \quad (1)$$

where X_c is the porosity. M_c and V_c are the mass and the volume of the specimen, respectively. M_s and V_s are those of the sacrificial core. ρ_{Al} is the density of aluminum. Eqution (1) was also used for the sintered specimens because the influence of the alloy layer on the porosity evaluation was negligible.

Subsequently, the sintered specimen was cut to thickness of 5 mm as shown in Fig. 3.

Then, the cut specimen was sealed by silicone coating with the exception of the microchannel.

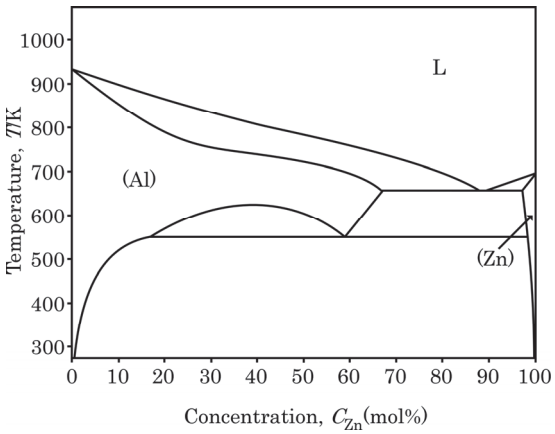

Fig. 1 Al-Zn binary alloy phase diagram [8]

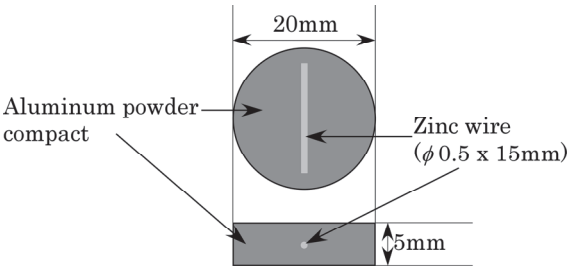

Fig. 2 Schema of the compact specimen

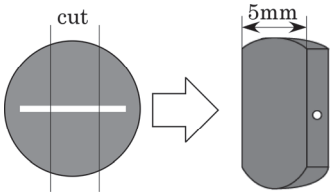

Fig. 3 Preparation of the specimen for anodic oxidation

2.2 Anodic oxidation of the specimens

The inner wall of the microchannel was anodized at room temperature at 50 V in the 0.22 kmol/m^3 oxalic acid solution. The anodic oxidation time, τ_a, was 1.8 ks. The specimen was used as the anode and a platinum plate was used as the cathode.

3. Results

3.1 Structure and composition of the specimen before anodic oxidation

Figure 4 shows the influence of the compacting pressure on the porosities of the specimens before and after sintering. Each porosity of the specimen decreased as the compacting pressure increased. Figure 4 also indicates that the porosity of the sintered specimen is slightly higher than that of the green compact prepared under the same pressure. Probably, strong oxide films covering the aluminum powder particles prevented densification of the specimens during heat treatment.

Figures 5(a), 6(a) and 7(a) show cross-sectional structures near the microchannels. Figures 5(b), 6(b) and 7(b) show results of EPMA. An open microchannel is produced for each compacting pressure. No major difference is observed in the structure near the microchannel nor in the composition of the lining layer. The average diameter of each microchannel was about 1000 μm or more and the zinc concentration in each lining layer was less than 15 mol%.

According to the Al-Zn binary alloy phase diagram (Fig. 1), the equilibrium liquid composition at 873 K is Al-18mol%Zn. Extension of the cross-sectional area of the microchannel was probably caused by dissolution of the aluminum powder particles surrounding the sacrificial-core metal pool. This problem can be solved by smooth migration of the sacrificial-core metal. Control of the porosity of the compact specimen may be a solution.

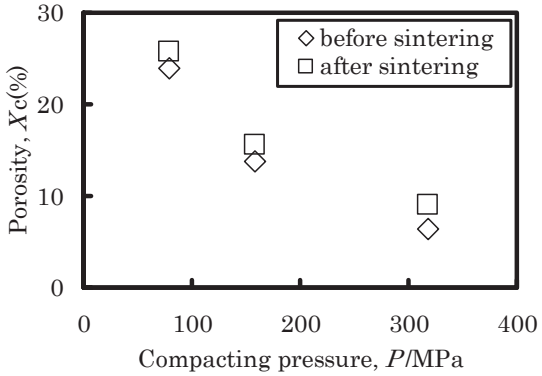

Fig. 4 Porosities of the compact specimen before and after sintering

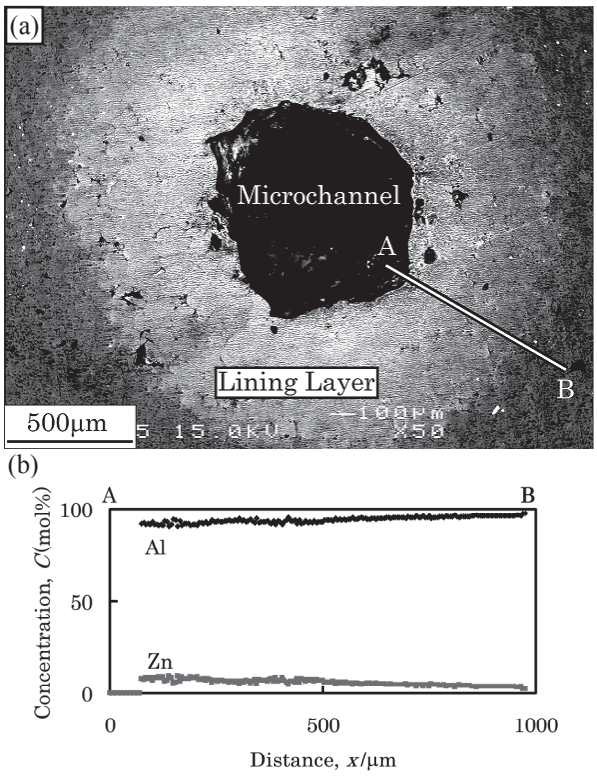

Fig. 5 SEM image near the microchannel produced in the specimen pressed under 79.5 MPa (a) and the concentration profiles along the line A-B (b)

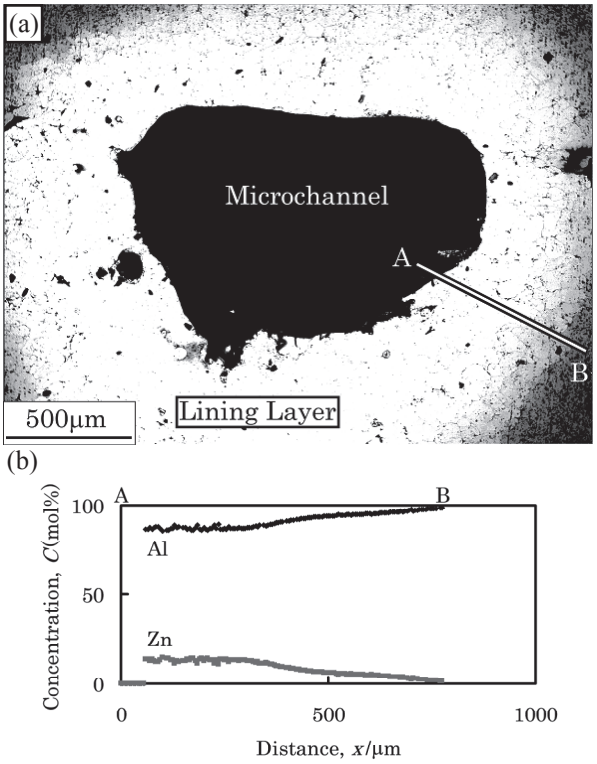

Fig. 6 SEM image near the microchannel produced in the specimen pressed under 159 MPa (a) and the concentration profiles along the line A-B (b)

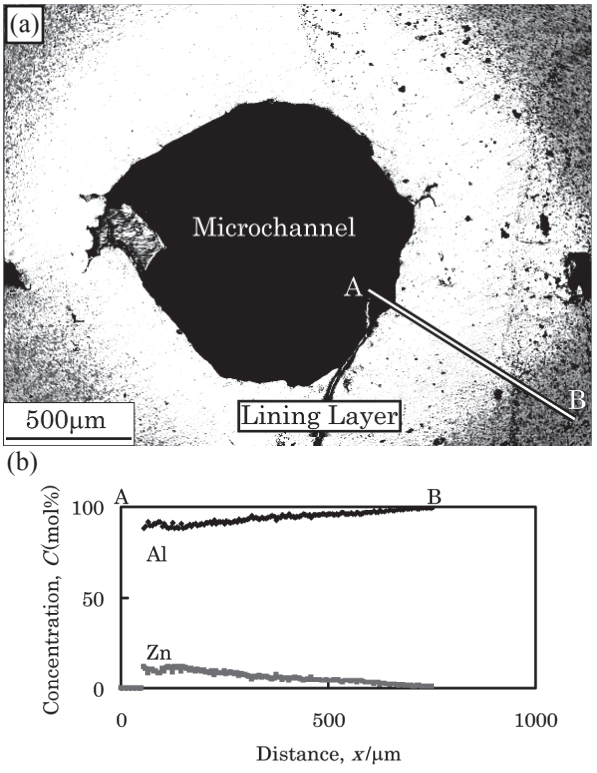

Fig. 7 SEM image near the microchannel produced in the specimen pressed under 318 MPa (a) and the concentration profiles along the line A-B (b)

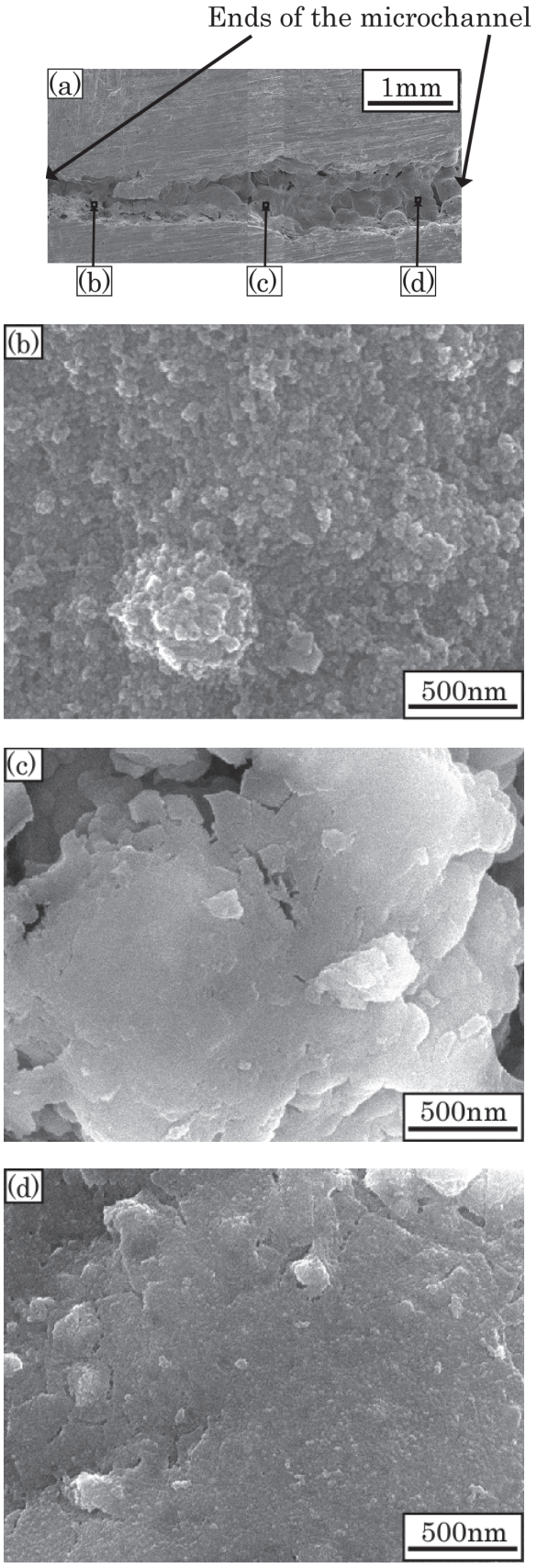

Fig. 8 Structure of the inner wall of the microchannel after anodic oxidation in the specimen pressed under 79.5 MPa. (a) Longitudinal section of the microchannel. (b)-(d) Structures of the anodic oxide film

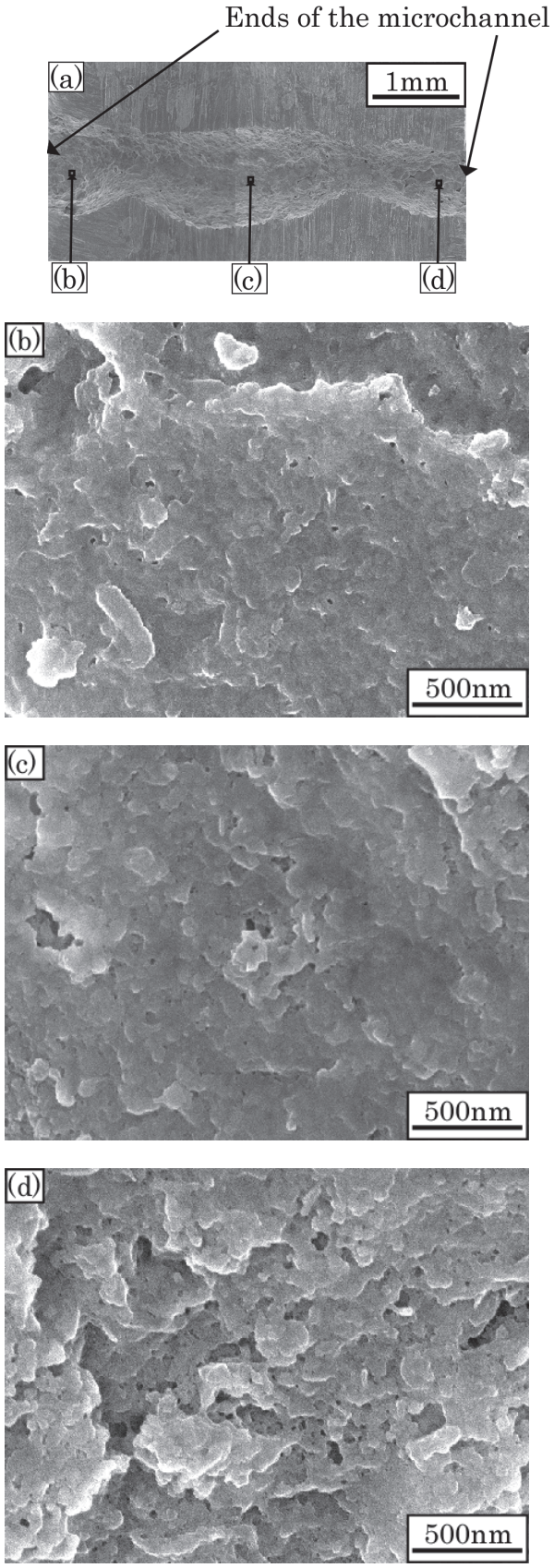

Fig. 9 Structure of the inner wall of the microchannel after anodic oxidation in the specimen pressed under 159 MPa. (a) Longitudinal section of the microchannel. (b)-(d) Structures of the anodic oxide film

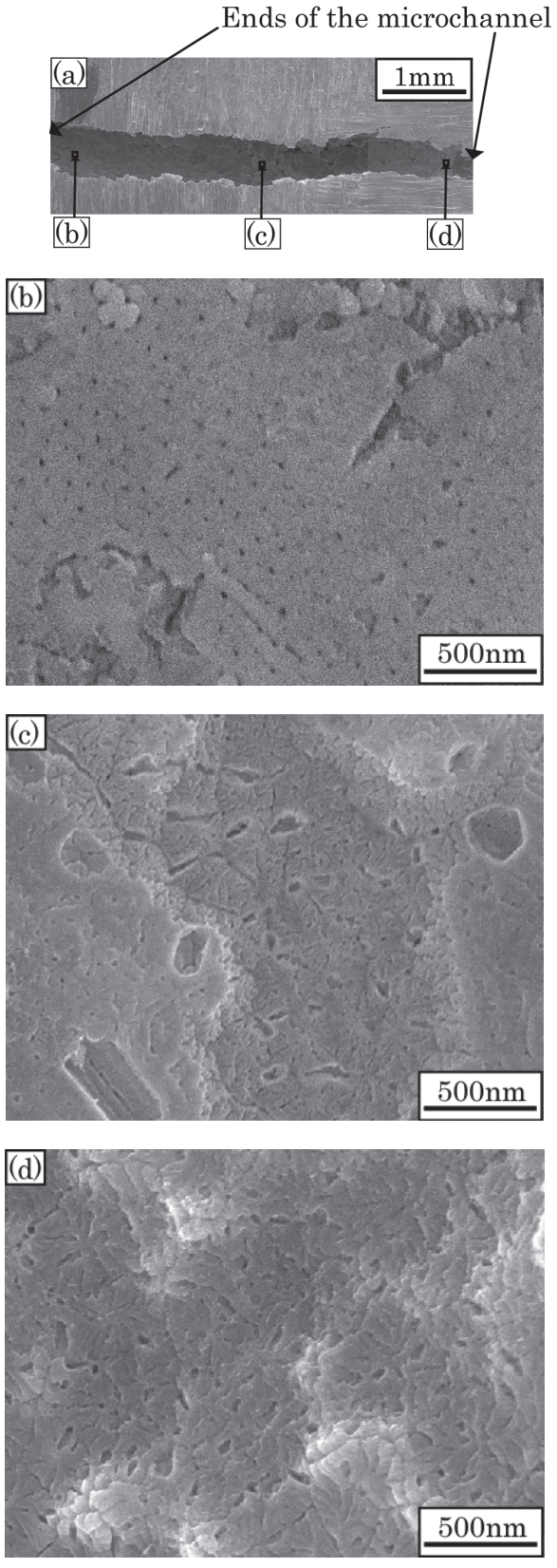

Fig. 10 Structure of the inner wall of the microchannel after anodic oxidation in the specimen pressed under 318 MPa. (a) Longitudinal section of the microchannel. (b)-(d) Structures of the anodic oxide film

3.2 Structure of the specimen after anodic oxidation

Figures 8-10 show the surface structures of the inner wall of the microchannels after the anodic oxidation.

In the specimen pressed under 79.5 MPa (Fig. 8), no aligned nanoporous structure was observed. Instead, nanoscale asperity was produced. In the specimen pressed under 159 MPa (Fig. 9), the anodic oxide film seems to have embryotic nanopores. On the other hand, fine nanopores can be seen in the specimen pressed under 318 MPa (Fig. 10).

According to the potential-pH diagram, Zn^{2+} was stable in this anodizing condition. Therefore, the anodic oxide film probably consisted of Al_2O_3 [9]. The detailed reason is not clear why the anodic oxide film did not become porous in the specimen with high porosity. Possible causes of the results are the microscale asperity on the inner-wall surface of the microchannel and the mechanism of the anodic oxidation of Al-Zn alloy. In the course of the anodizing, dissolution of zinc occurred before full-fledged oxidation of aluminum. In addition, the inner-wall surface of the microchannel in the high-porosity specimen had a high specific surface area. Therefore, such a specimen required a long time for the step of zinc dissolution. As a result, anodic oxidation treatment was finished before formation of the nanoporous oxide film.

4. Conclusions

Fabrication of the nanoporous oxide film on the inner wall of the microchannel produced by a sacrificial-core method was examined. The results obtained are summarized as follows.

(1) The open microchannel was formed in each specimen compacted under 79.5, 159 or 318 MPa.

(2) The compacting pressure affected the porosity of the green compact but not significantly on the composition of the microchannel lining layer.

(3) The nanoporous anodic oxide film was produced on the inner wall of the microchannel in the specimen with low porosity, about 8.1%, but not in the specimen with higher porosity.

References

[1] Hibara, A.: Microchemistry and Micro Two-phase Flow, *Japanese J. Multiphase Flow,* **23**-2 (2009) 129-134.

[2] Ishida, M., Ohmi, T., Sakairi, M. and Iguchi, M.: Formation of Nanoporous Anodic Oxide Films on Ti-Al Microchannel Walls, *Journal of JSEM*, **10** Special Issue (2010), 210-214.

[3] Ohmi, T., Sakurai, M., Matsuura, K. and Kudoh, M.: Formation of Microchannels in Sintered Titanium-Powder Compacts by Local Reactive Infiltration, *Proc. 15th Int. Symp. on Trans. Phenomena*, (2004), 364-367.

[4] Ohmi, T., Matsuura, K. and Kudoh, M.: Formation of Intermetallic-Lined Microchannels in Sintered Metals by Local Reactive Infiltration, *Int. J. Self-Propagating High-Temperature Synthesis*, **13**-2 (2004), 121-129.

[5] Ohmi, T., Takatoo, M., Iguchi, M., Matsuura, K. and Kudoh, M.: Powder-Metallurgical Process for Producing Metallic Microchannel Devices, *Mater. Trans.*, **47** (2006), 2137-2142.

[6] Ohmi, T., Sakurai, M., Matsuura, K., Kudoh, M. and Iguchi, M.: Formation of Microchannels in Sintered Titanium-Powder Compacts by Microscopic Reactive Infiltration, *I. J. Trans. Phenomena*, **9**-2 (2007), 105-111.

[7] Ohmi, T., Takatoo, M., Iguchi, M., Matsuura, K. and Kudoh, M.: Fabrication Process for Metallic Microchannel Devices for High-Temperature Use, *Journal of JSEM*, **5**-3 (2005), 40-44.

[8] Murray, J.L.: The Al-Zn (Aluminum-Zinc) system, *Bull. Alloy Phase Diagrams*, **4** (1983), 55-73.

[9] Pourbaix, M.: Atlas of Electrochemical Equilibria in Aqueous Solutions, *NACE International Cebelcor*, (1974), 409